



The Submerged Arc Furnace (SAF): State-of-the-Art Metal Recovery from Nonferrous Slags

Bernd Friedrich¹ · Michael Kalisch² · David Friedmann¹ · Rolf Degel² · Frank Kaußen¹ · Jörn Böhlke¹

© The Minerals, Metals & Materials Society 2018

Abstract

The submerged electric arc furnace (SAF) has proven a versatile unit in numerous metallurgical applications for more than a century. Countless innovations have made this furnace type become the most commonly used furnace for increased metal recoveries and slag-cleaning operations. In many applications, SAFs are also employed as primary melting units (e.g., Ni Laterites, Si production, FeMn, FeCr, etc.). Furnace power supply as well as capacities has been continuously increased over the years so that modern SAFs can reach more than 100 MVA as well as more than 100 tph in throughput. The present paper aims to provide a thorough overview of the principles and buildup of modern SAFs and to present various examples from recent industrial installations as well as current topics in pyrometallurgical research. Examples of the buildup and special equipment (such as cooled wall panels, Soderberg electrodes, etc.) of modern SAFs are demonstrated. The paper also presents metallurgical, thermochemical, and physical fundamentals of slag cleaning as well as particle settling. Furthermore, industrial examples from two African sites are discussed, which highlight the advantages of the SAF for metal recoveries. Special emphasis is given to an innovative slag-cleaning concept through magnetic agitation. Research topics presented range from the inertization of red mud, to Co recovery through the retreatment of dumped slag and the valorization of Pb- and Zn-containing slags.

Keywords SAF · Submerged-arc-furnace · Slag-cleaning · Slag-washing-machine · Cobalt-recovery · Redmud

Introduction

In metallurgical production, the traditional aim is to increase recovery of metal to the maximum. It becomes apparent that the application of the submerged arc furnace (SAF) in nonferrous metallurgy processes is increasing, in particular for the extraction of zinc, lead, copper and

nickel, but also for the processing of residues and stripping of slag. The SMS group has been developing this technology for 100 years, and has supplied a diverse market with about 700 furnaces and major furnace components [1]. During this time, numerous applications were continuously being developed in order to serve the demands of various users [2]. Especially more than 20 slag-cleaning furnaces have been supplied in the last 40 years. Slag-cleaning furnaces are commonly connected to smelting units such as Teniente and Noranda converter, Outokumpu flash smelter, reverberatory furnaces, etc. The main function of the furnace is the reduction of the matte and metal level in the slag. Depending on the upstream process, the slag is either liquid-charged via launders into the furnace or is cold-charged in solid form via conventional feeding systems.

Principle of SAF

The SAF works with electric energy which is converted into heat, mainly using the electric resistance of the burden or molten slag. The electrodes are immersed in the melt

The contributing editor for this article was Annelies Malfliet.

✉ David Friedmann
dfriedmann@ime-aachen.de

Bernd Friedrich
bfriedrich@ime-aachen.de

Michael Kalisch
michael.kalisch@sms-group.com

Rolf Degel
rolf.degel@sms-group.com

¹ IME Process Metallurgy and Metal Recycling, RWTH Aachen University, Intzestr. 3, 52072 Aachen, Germany

² SMS Group GmbH, Eduard-Schloemann-Straße 4, Düsseldorf 40237, Germany

which provides the required energy exchange area between electrode and melt. The melt is the heat exchange medium which supplies the energy required for melting and chemical reactions of the charge [3]. The submerged arc furnace comprises the following major equipment parts as seen in Fig. 1.

A typical furnace with slag operation comprises a round or rectangular furnace shell with tap holes for slag, matte or metal. The furnace shell is refractory lined and—if additional shell cooling is required by the process—water-cooled. Various sidewall cooling systems are available depending on the specification of the process: rinse cooling, spray cooling, chamber cooling, chanel cooling or Cu-strip cooling (see Fig. 2). For safety reasons, the cooling chanel s remain outside the furnace shell. In certain applications such as Platinum Group Metals (PGM), pig iron and several ferroalloys and nonferrous processes, a sufficient heat-removal rate will create a layer of frozen slag, the so-called “freeze line,” which protects the remaining sidewall lining. In this case, a high thermal conductivity of the lining is of capital importance.

The shell bottom is cooled, if cooling is necessary, by forced air ventilation. In special applications, water cooling may be required. Furnace roofs, either brick type or water-cooled type, comprise all required glands, openings, and sealings for the electrode columns, charging pipes, and off-gas ducts.

The electric energy is transferred into the furnace via self-baking carbon electrodes or prebaked graphite electrodes. The electrode arrangements are depending on the process and the installed power. They are arranged either centrally (single electrode) or as triangle (three electrodes); in case of a rectangular furnace, they are arranged either as 3 or 6 electrodes along the centerline as 2 lines with 3 electrodes each. Therefore, one of the key components of the furnace is the electrode column (see Fig. 3).

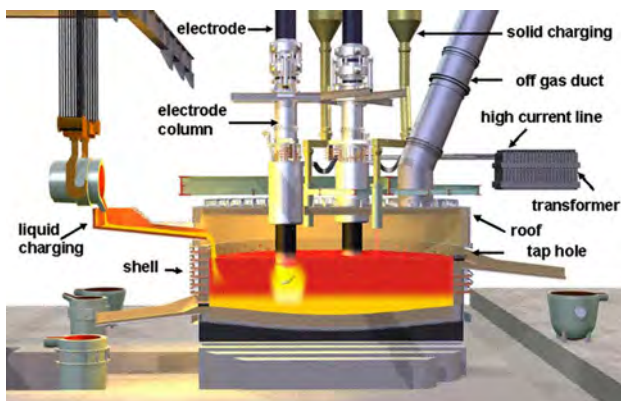


Fig. 1 Main components of a submerged arc furnace [3] (Color figure online)

The electrode is semiautomatically slipped into the bath, carried out under full electric furnace load with no interruptions to furnace operation. The electrode column assemblies contain all facilities to hold, slip, backslip, and regulate the penetration into the bath. All operations on the electrodes are executed hydraulically.

The electric power is normally transferred from the furnace transformers via high current lines, water-cooled flexibles, bus tubes at the electrodes and the contact clamps into the electrodes. Today the control and supervision are implemented by a Programmable Logic Controller (PLC) and visualization system. A back-up for manual operation is foreseen and is located in the control room [4].

Metal, slag or matte are tapped periodically by means of a drilling machine and closed either with a manually placed plug or a mud gun. Metal is tapped in ladles, slag/matte is either tapped into slag pots, dry pits or granulation systems (see Fig. 4).

The process gas created from the chemical reactions is provided at the gas stack connection at the furnace roof. Depending on the plant design, the process gas is combusted either inside of the furnace or outside the furnace by balanced addition of combustion and cooling air and sent to the filter system. If the process generates off-gas which contains a certain amount of CO in the process gas or other hazardous substances, the furnace is designed as a closed furnace type.

The above described furnace type is considered to be a typical design. Various other layout/design options meet the individual requirements of specific processes. Successful operation is always based on the right choice of furnace design and furnace dimensions. The choice of the raw material according to the customer's aspects has the biggest impact on the process. On the one hand it affects the slag composition and on the other hand the smelting pattern inside the furnace based on the physical properties and the amount of energy input.

Fundamentals of Slag Cleaning

Smelting slags can contain valuable metals in dissolved form and as mechanically entrained matte or metallic inclusions in the size range from 2 to 1000 μm . Conditions that encourage suspended matte droplet to settle to a matte layer are low viscosity slag, low turbulence settling, a long residence time, and a thin slag layer. These conditions are often difficult to obtain in a smelting vessel, particularly the necessary residence time.

Pyrometallurgical slag cleaning usually consists of heating the slag, reduction of oxides and settling of matte/metal droplets. Heating the slag decreases viscosity and accelerates reactions. Reduction of magnetite liberates

Fig. 2 Side wall copper stripe cooling [19] (Color figure online)

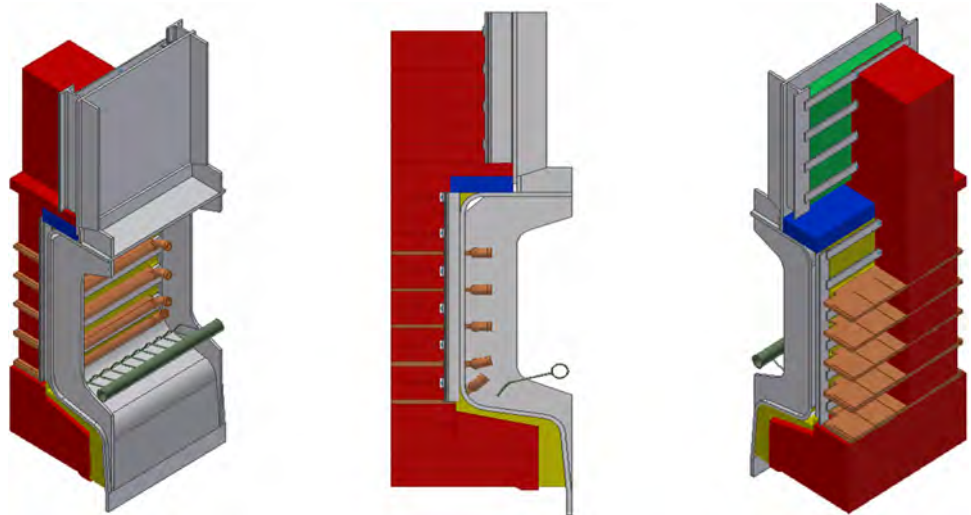


Fig. 3 Electrode column [4] (Color figure online)

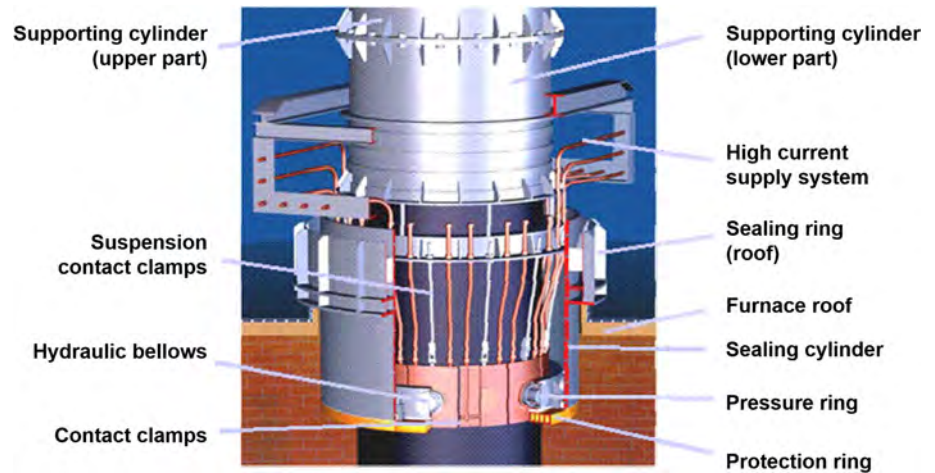


Fig. 4 3D illustration of a rectangular slag-cleaning furnace [19] (Color figure online)

inclusions and facilitates co-reduction of dissolved metal oxides. A significant amount of the matte and metal is

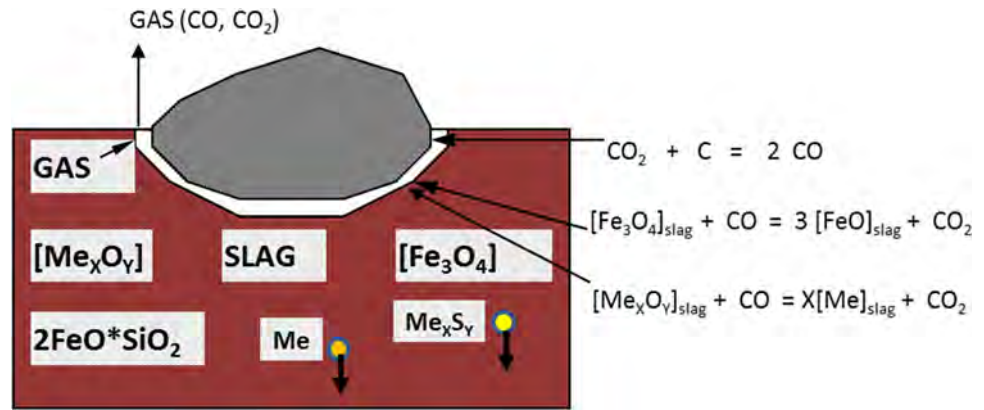
present as very fine metallic inclusions, too small for settling. The coalescence of these matte or metal inclusions is required to remove them from the slag.

Chemical Slag-Cleaning Process

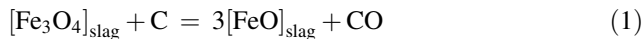
The metals in smelting and converting slags are present either dissolved, present mostly as ions (e.g., for copper slag as Cu^+ ions) or as entrained droplets of matte. The dissolved metals is associated either with O^{X-} ions (i.e., Cu_2O) or with S^{X-} ions (e.g., Cu_2S). Electric slag-cleaning furnace uses coke as a reductant. So, coke bed is floating on the slag surface and reacting with oxides. At the initial moment of the contact of carbon and slag the direct reduction reaction takes place, forming a gas film separating solid carbon and liquid slag phases as it is illustrated in Fig. 5.

At the coke/slag interface indirect magnetite (Fe_3O_4) reduction and Boudouard's reaction (CO/CO_2) take place, together with the reduction of metal oxide (Me_xO_y).

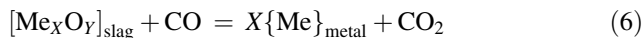
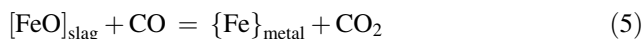
Fig. 5 Slag reduction with coke floating on its surface [5] (Color figure online)



Direct reduction



Indirect reduction



Boudouard reaction



Reducing viscosity can be achieved by increasing the slag temperature, and changing slag chemistry. The main focus of changing slag chemistry is to reduce the magnetite that is present within the slag, mainly according to Eqs. (1) and (4). Other reactions to reduce the magnetite content involve iron with higher carbon content (4–5%) and sulfides [5–7].

Physical Slag-Cleaning Process

Settling rate of spherical body in a liquid is described by Stokes's law:

$$u = \frac{2(\rho_M - \rho_S)gr^2}{9\eta_S} \quad (8)$$

Matte and metallic inclusions are present in a molten slag in the form of liquid droplets. The rate of settling of a liquid, spherical drop in a liquid is given by Hadamard–Rybczynski formula:

$$u = \frac{(\rho_M - \rho_S)gr^2}{3\eta_S} \frac{3\eta_S + 2\eta_M}{3(\eta_S + \eta_M)} \quad (9)$$

Because slag viscosity is much higher than matte or metal viscosity ($\eta_S \gg \eta_M$) the settling rate of matte and

metallic inclusions in the slag can be calculated using the modified Hadamard–Rybczynski formula for slag/matte system:

$$u = \frac{(\rho_M - \rho_S)gr^2}{3\eta_S} \quad (10)$$

The wide range of sizes of inclusions, varying from 2 to 1000 μm , and differences in the settling rates of different sized droplets cause the droplets to collide and coalescence, called gravitational coalescence. The bigger droplets “wash out” the smaller ones by absorbing them as the big droplets fall faster through the slag than small ones do [8]. It requires precise information about size distribution of matte and metallic inclusions. E.g., based on the microscopic examination of the slag of 3.5% copper content from Teniente Converter a typical size distribution of copper matte inclusions and metallic copper inclusions are shown in Figs. 6 and 7 [6, 9].

In Fig. 8, the curve for calculation of the copper content with only gravitational settling (Eq. 10) is given. After 2 h, the copper content is close to 2%. Also, the copper content

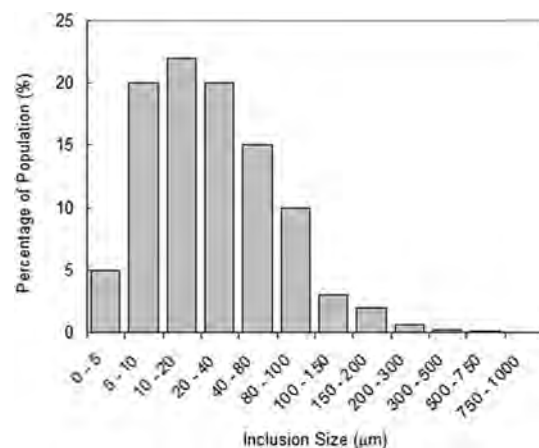


Fig. 6 Size distribution of copper matte inclusions in slag form Teniente Converter [20]

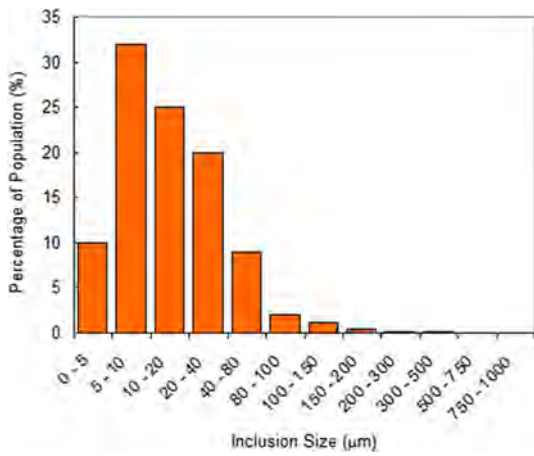


Fig. 7 Size distribution of metallic copper inclusions in slag form Teniente Converter [20] (Color figure online)

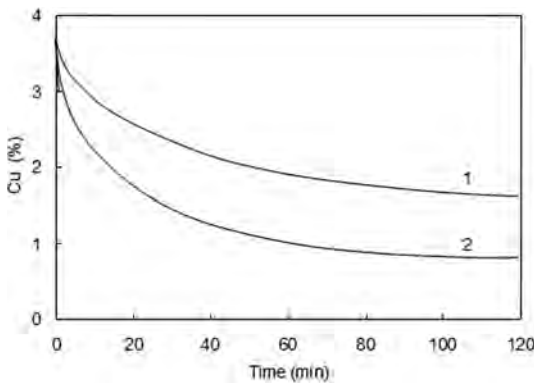


Fig. 8 Calculated copper content in the form of matte inclusions versus time 1 gravitational settling, 2 gravitational coalescence

was calculated using the gravitational coalescence model (Fig. 8—Curve 2).

If the droplets are too small, then settling takes a lot of time. This can be counterbalanced by allowing a long settling time, and by reducing the viscosity of the slag. A longer settling time is achieved by properly designing the furnace, but there are limits to the practical size of a furnace. The principle of the model of gravitational coalescence is schematically shown in Fig. 9. Every settling droplet creates an “attraction volume” in the period of time Δt . The attraction volume is a function of inclusion diameter, settling rate and time. Assuming homogeneous distribution of inclusions in the slag, the average, maximal settling distance is equal to half of the slag height.

$$V_i = \pi r_i^2 u_i \Delta t \tag{11}$$

The moment the bigger and smaller droplet collide, the bigger droplet “absorbs” the smaller one and the size of bigger droplet increases.

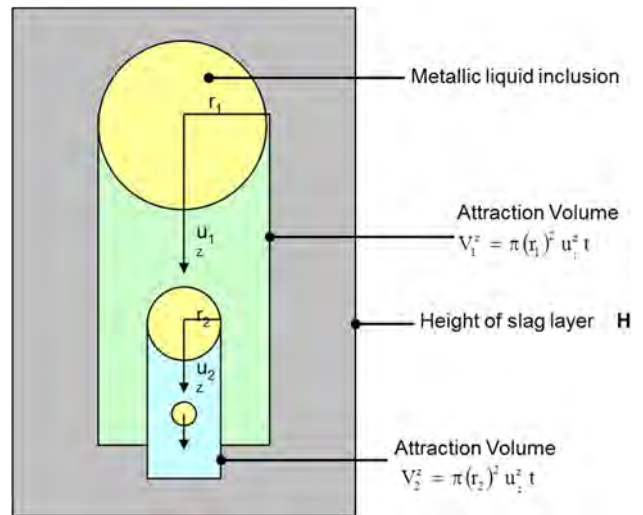


Fig. 9 Gravitational settling and coalescence of matte inclusions in the slag [20] (Color figure online)

$$r_i^{k+1} = \sqrt[3]{(r_i^k)^3 + \beta V_i \sum_{j=1}^{i-1} n_j^k (r_j^k)^3} \tag{12}$$

The effectiveness of coalescence depends on the number of collisions and interfacial tension. The empirical coefficient β represents the coalescence effectiveness on a scale of 0–1.

The passing of inclusions from slag to the matte layer and the coalescence results in the change of inclusions number in all size fractions. In the iteration step Δt (number k), the number of inclusions size i is defined by formula:

$$n_i^{k+1} = n_i^k \left[\left(e^{-\frac{u_i}{H} \Delta t} \right) + \left(1 - \beta \sum_{j=1}^{i-1} n_j^k (r_j^k)^3 \right) \right] \tag{13}$$

Finally, the metal content (in the form of matte inclusions) in the slag at time t , corresponding to iteration number k , is calculated by summarization of all matte inclusions in the unitary volume of slag, assuming that the metal content in the matte inclusions is equal to metal content in produced matte [8].

$$Me_M^k = \frac{4}{3} 10^4 \pi \frac{1}{Me_{CM}} \frac{\rho_M}{\rho_S} \sum_{i=1}^m n_i^k (r_i^k)^3 \tag{14}$$

Similarly the gravitational coalescence of metallic inclusions has been calculated, their size distribution have to be based on microscopic examination. The total metal (Me_T) content at iteration step k is equal to the sum of contents of metal in the form of matte (Me_M), metallic (Me_{CM}) and metal oxide (Me_O) [5, 6, 9]:

$$Me_T^k = Me_M^k + Me_{CM}^k + Me_O^k \quad (15)$$

Exemplary Results and Industrial Applications

Copper Slag Cleaning in First Quantum at Kansanshi Copper Smelter

Copper slag cleaning in (electric) furnaces has become increasingly popular over the recent decades. METIX, part of the SMS group, has recently constructed an electric furnace for the First quantum project at Kansanshi, Zambia. The plant was commissioned successfully in February 2015 (see Fig. 10).

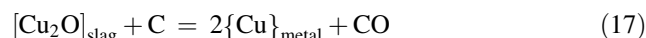
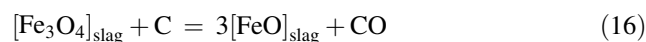
First Quantum Minerals Limited was already a major producer of SX-EW (Solvent extraction and electrowinning) copper at their operating unit in Kansanshi, Zambia when they chose to expand their operation by installing a copper smelter. An ISASMELT was chosen for the smelting furnace application. The new smelter concept with a downstream Matte Settling Electric Furnace promises to provide a major benefit. The Kansanshi Smelter is producing 300,000 tons per annum of blister copper from a concentrate blend based on feed from the Kansanshi and Sentinel mines by treating up to 1.2 million dry t/y copper concentrates.

There is an increasing trend toward adopting semicontinuous operating practice of the primary smelters (such as ISASMELT or Ausmelt) as well as of the slag-cleaning

furnaces. The rectangular SAF is more suitable for this task due to its better geometric features. It is expected that for continuous operation, the recovery rate of a rectangular furnace can reach (depending on the specific parameters) 0.1–0.4% higher in comparison with the conventional cylindrical-type SAFs. This fact motivated First Quantum to install at Kansanshi copper smelter in Zambia a six-in-line rectangular slag-cleaning furnace of 12.5 MW downstream a continuously operating ISASMELT furnace [2].

Slags obtained from the smelting of sulfide concentrates contain between 2 and 10% of copper, which are present in dissolved form and as matte inclusions with the size ranging from 2 to 1000 μm . The Matte Settling Electric Furnace (MSEF) is capable of processing copper matte, various converter slags, reverts from different sources and coke to produce a slag with a maximum copper content of 0.7%. The MSEF at Kansanshi is continuously charged via two launders with matte and slag coming from the ISASMELT. The launders enter the furnace shell in the gas area through the sidewall and are positioned to convey the slag directly into the reaction area to prevent the precipitation of a major quantity of magnetite. Molten slag from the PSC is charged by ladle at regular intervals into the furnace by means of two dedicated cast iron launders in the eastern end wall from the converter aisle side. A mixture of reverts, coke, and limestone is fed through the feed chutes into the furnace on top of the molten slag layer in the furnace. The coke and limestone act as modifiers to the slag to improve conductivity and viscosity to facilitate the copper matte settling in the furnace, while reverts are fed back to ensure recovery of contained copper.

As mentioned above, the settling will be achieved by temperature increase and reduction of copper oxides and magnetite in the slag with carbon and maximizing of the settling rate of the metallic or matte droplets by improving the viscosity of the slag. It is commonly agreed that reduction of oxides from a liquid slag with carbon



is the first-order reaction with respect to the oxide concentration, so the rate of magnetite reduction is represented by equation:

$$\frac{dC_{\text{Fe}_3\text{O}_4}}{dt} = k \frac{A_R \rho_S}{m_S} C_{\text{Fe}_3\text{O}_4} \quad (18)$$

where A_R represents reaction surface area, and m_S/ρ_S ratio represents the slag volume. Value of reaction constant k as the function of temperature has been determined experimentally by reduction of slag with coke.

When reaching the fayalite point with approximately 29% of SiO_2 , the viscosity of the slag shows a maximum

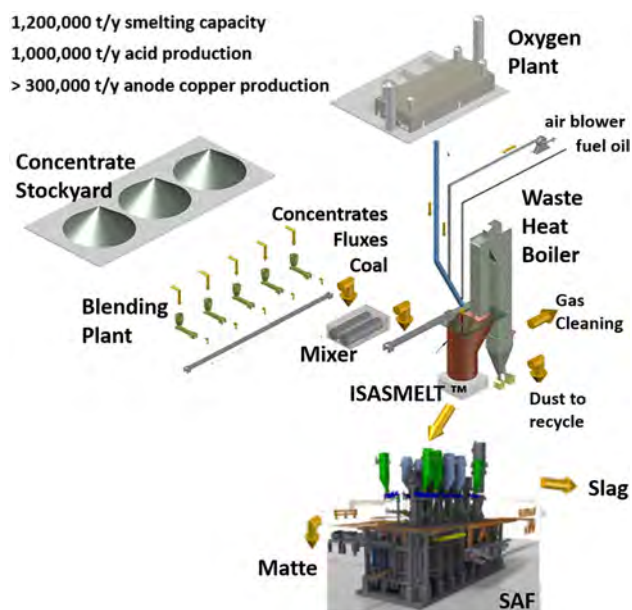


Fig. 10 3D illustration of Kansanshi copper smelter (Color figure online)

value. A slag with 30–33% SiO_2 will lead to poor slag-cleaning results as it is very difficult for Cu and Cu matte droplets to settle. This is one of the reasons to keep the magnetite content within the range of 4–6%. Figure 11 shows representative results of discarded slag with the correlation between magnetite and total Cu content in MSEF slag.

Tapping of the furnace is done through eight matte tap holes all situated on the same level and on both the north and south sides. The matte tap holes are equipped with a rail mounted mud gun and drill on each side of the furnace to assist with opening and closing of the tap holes. The tapped MSEF matte is ladled to Peirce-Smith converters, and the MSEF slag will be granulated and discarded.

Latest Results from Pilot-Scale Operation: Highly Efficient Slag Cleaning

Conventional pyrometallurgical slag-cleaning process by submerged arc furnaces comprises slag heating, reduction of oxides, and settling of matte/metal droplets. Slag overheating decreases its viscosity and accelerates reduction reactions. By applying a magnetic field crossing a DC field to a slag, stirring can be improved and the settling of entrained copper droplets is thereby fostered. Based on this theoretical background and on the results of an intensive parameter study by CFD simulation, the results were subsequently verified in a 2–4 t/h pilot plant. [10]

The background is that the given process conditions only allow copper particles to settle if they are above a certain minimum size. As a result, the smaller copper sulfide droplets included in the iron silicate product (the real constituent of the slag) remain, which means that the economic use of the valuable metal content becomes

impossible. The new process combination is intended to separate the remaining metal phase from the slag. This combination envisages that a stirring reactor with induced magnetic, activated “washing” (stirring) will be installed downstream of the already established submerged arc furnace. The relevant patent drawing for this process is depicted in Fig. 12 [11].

Physically, the Lorenz force is used. This works on metal particles if they are in a DC electric field which is crossed at right angles by a magnetic field. The copper particles are subjected to a rotary motion, which causes impact and agglomeration due to different velocities of the particles, and then after acquiring increased mass, they can settle down [12].

The new process and furnace concept have been tested extensively. Two pilot plants were built for smaller and larger laboratory trials at the University of Chile and a small test facility in Charges in Chile. After these promising but short-term test campaigns, a small plant was installed at the Institute of Metallurgy, Recycling and Process Engineering (IME) at the RWTH University of Aachen, to primarily serve the scientific purposes of the university. Furthermore, finally a large pilot plant was erected, fully integrated into an industrial company involved in copper production at Aurubis, Hamburg. The pilot plant in Hamburg was operated in test campaigns. The duration of each campaign was 8–10 days, including the heat-up phase for 2–3 days and the operating period. During the operating period, the furnace was fed with slag from the industrial slag-cleaning furnace semicontinuously. Figure 13 shows some illustrations of the pilot-scale operation [12].

Each test campaign, except the last one, includes a time period for slag treatment in the stirring reactor without

Fig. 11 Kansanshi MSEF discarded slag assays CW16 2015 (Color figure online)

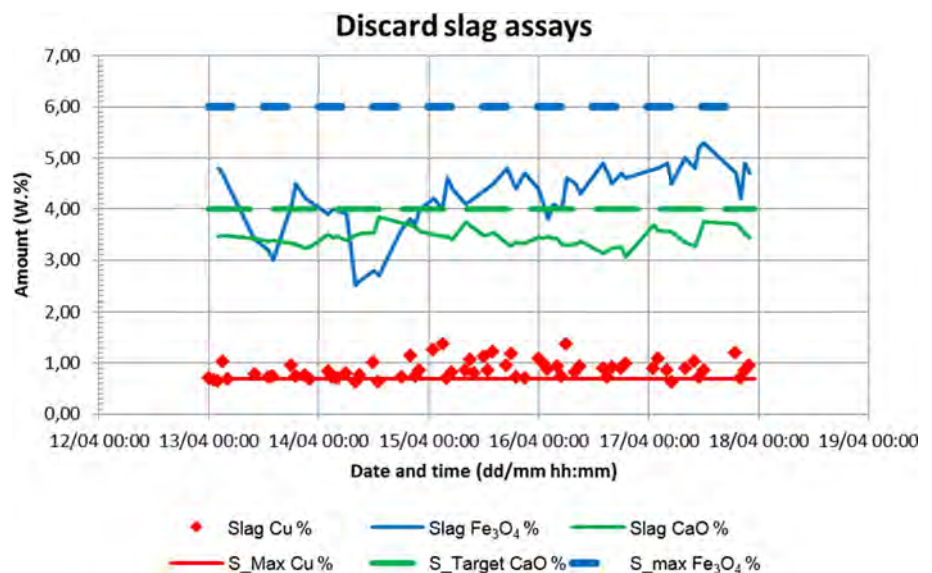


Fig. 12 Patent drawing SMS group [11]

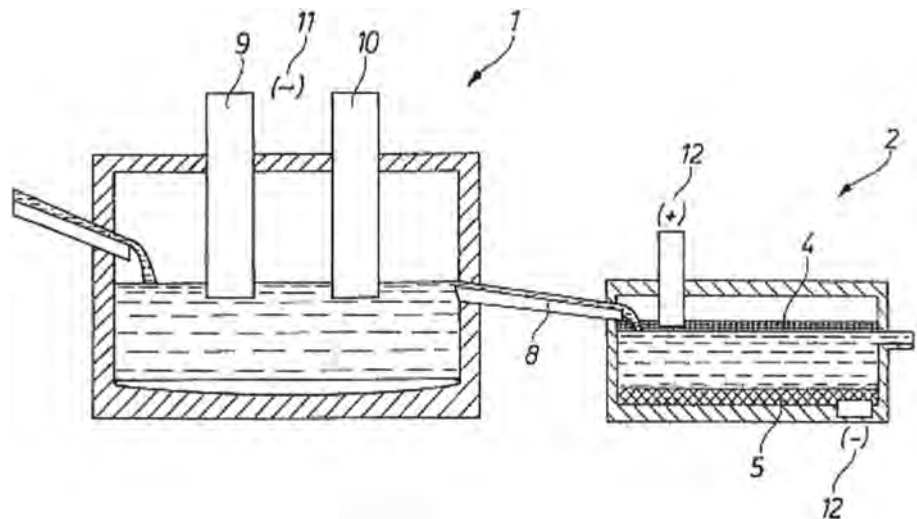


Fig. 13 Pilot plant at Aurubis Hamburg [12] (Color figure online)

magnetic stirring in order to obtain the reference value of copper separation. In terms of the application of the magnetic stirring device, the position of the magnetic poles, the operating mode, and magnetic force were investigated.

All samples from the pilot plant at Aurubis Hamburg were taken directly from the overflowing mass-flow at a certain time after the first overflow of slag phase and were granulated in water. To evaluate the relative efficiency of copper separation, a comparison to a reference status without any enhanced magnetic stirring is required. As

there are also present certain minor effects like slag temperature of the feed and overflow as well as retention time and several others, the obtained results are illustrated in the form of histograms [12].

Figure 14 shows the histogram for the results obtained without enhanced stirring and with applied enhanced stirring. Since the copper separation depends on the copper concentration of the feed material, it is necessary to compare both measurement series with respect to average and standard deviation before determining the differences in

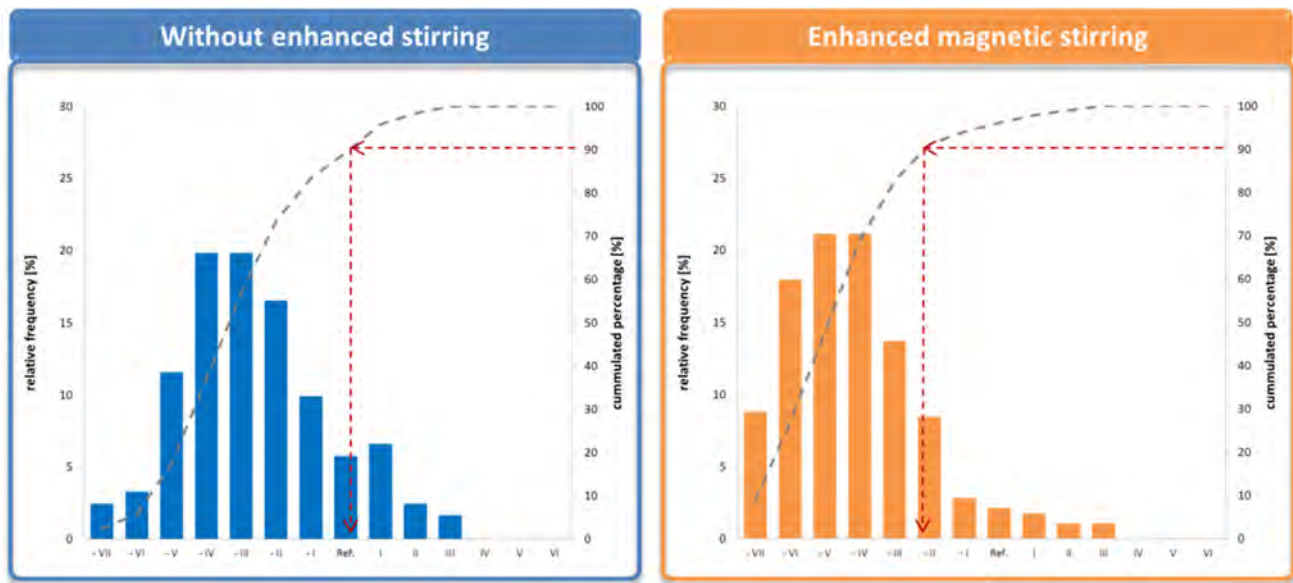


Fig. 14 Comparison of results obtained without enhanced stirring to those with applied enhanced stirring [13] (Color figure online)

the achieved results. The comparison of these two parameters showed no significant deviation between the two investigated states [13].

The graph for the enhanced magnetic stirring shows an accumulation of values in the classes V and below. The relative frequency of copper concentration in the iron silicate product is nearly tripled compared to the status without enhanced stirring to 47.9% of the investigated charges. In general, the results obtained during the application of the magnetic field show a smaller variety of the achieved Cu concentration in the overflow. The red dotted line illustrates the difference between the cumulative percentages for both measurement series. Assuming that the reliability of the gained copper concentration of 90% would be sufficient for industrial operation, it is evident that without enhanced stirring, the results are comparable to the reference state and it would need the enhanced stirring to achieve even better results. Summarizing these results, it can be stated that the application of a magnetic field led to a significantly lower copper concentration in the remaining iron silicate product [13].

To demonstrate the effect of copper feed content on the remaining copper content in the final iron silicate product, Fig. 15 illustrates the average copper separation. For the histogram, the copper feed content was classified according to the above-mentioned procedure, and the average copper separation was determined for each process mode, on the one hand, and for each histogram class, on the other hand [12].

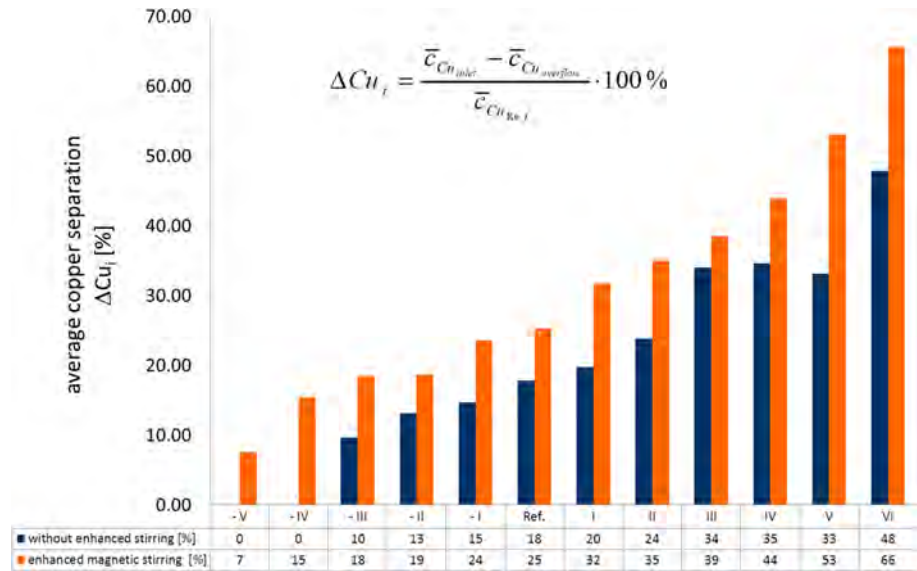
The driving force of separating copper from the feed material increases with a rising copper concentration. This means that even at high copper concentrations in the feed,

sufficient separation to low copper concentrations in the overflow iron silicate product is feasible. On determining the copper separation ratio between the enhanced stirring status and the status without stirring, the value is > 1 for every histogram class. This means that independent of the copper concentration of the feed material, the application of the magnetic field leads to a better copper separation than the reference status without enhanced stirring. Even at low copper concentrations (IV, V) in the feed, copper can be separated by applying the magnetic field, while this was not observed in the case without the enhanced stirring [12].

Reduction Smelting of Red Mud [14]

Red mud is the so-called bauxite residue after the solid–liquid separation from alkaline high-pressure leaching of aluminum bearing bauxite ore. Depending on the composition of the primary mineral deposit, 4–7 tons of bauxite are necessary to yield 2 tons of alumina in order to produce 1 ton of aluminum. The leaching process is very selective on the extraction of aluminum and gallium, and the undissolved minerals remain in the residue. Due to its high hematite content, the bauxite residue has a reddish color and is therefore called red mud. With each ton of primary produced aluminum, 1–2.5 tons of red mud are generated. The composition of red mud varies strongly depending on the composition of the original bauxite and the employed process parameters (digestion temperature, caustic concentration, digestion time, etc.). Table 1 shows the average ranges in composition of the commonly produced red muds. It can be seen that the predominant phases are iron

Fig. 15 Comparison of results obtained without enhanced stirring to those with applied enhanced stirring [12] (Color figure online)



compounds like hematite or goethite which can be easily recovered by carbothermic reduction.

The examined red mud comes from the landfill of the former “Vereinigte Aluminiumwerke” near Lünen, Germany. The original composition is shown in Table 1, and indicates high amounts of remaining alumina. In former times, high throughputs and cheap but poorly digestible bauxites as raw material did not lead to high alumina recovery. Therefore, X-ray diffraction patterns show the predominant phases are hematite and still aluminum hydroxides (gibbsite and boehmite). The exact aluminum content is measured by X-ray fluorescence, and the aluminum values in Table 1 are converted into alumina as quite commonly described in literature. The sum of all components does not make up 100%. This original red mud from landfill is one material for the following test trials.

Moreover, the entire research project includes a recovery of the maximum amount of the remaining alumina content. Therefore, the red mud from the landfill is leached a second time employing the Bayer process with optimized

parameters. From this second leaching originates a red mud with the composition called after “re-leaching” (see Table 1) which is also examined for iron recovery.

The third examined raw material for carbothermic iron recovery experiments is presented in the last column of Table 1. In this case, small amounts of lime are added during the second leaching of the initial red mud in order to increase the recovery of alumina in the leaching step. Experiments confirmed an increased alumina yield of about 10% since the molar ratio CaO/SiO₂ increased from 0.31 in the initial red mud to 0.5 by the addition of lime. Thus, the remaining leaching residue is increased in its lime content, while the other constituents are slightly diluted.

Theoretical Considerations

It can be seen from Fig. 16 that the hematite is first reduced to FeO. At about 15 g carbon addition, the co-reduction of titania to Ti₂O₃ starts but stagnates at a low level. Only 15–35% of the titania is reduced to Ti₂O₃. By adding 26 g

Table 1 Compositions of different red muds and composition of the raw material used in the experiments

Component in wt%	Average red mud	Red mud Lünen (Germany)	After re-leaching	After re-leaching with CaO (CaO/SiO ₂ ~ 0.5)
Fe ₂ O ₃	30–50	29.5	35.5	34.7
Al ₂ O ₃	10–20	27	18.3	17.7
SiO ₂	5–20	13.1	14.9	15
TiO ₂	3–15	8	9.3	9
Na ₂ O	3–7	7	9.3	9.1
CaO	1–8	3.8	4.7	7.7
Cr ₂ O ₃	–	0.35	0.41	0.4
P ₂ O ₅	–	0.22	0.25	0.27
SO ₃	–	0.47	0.5	0.58

carbon per kg re-leached red mud, the hematite is almost completely (remaining Fe_2O_3 content < 0.9 wt%) converted into FeO. If the addition of the reducing agent is further increased, a phase of metallic iron will be produced, and the FeO content of the slag declines. At about 80 g carbon addition, the FeO activity descends rapidly and the titania activity increases dramatically which leads to a significant titania reduction. At 87.5 g carbon addition, the iron oxide content in slag is less than 1 wt% so the reduction is completed. The metal phase first forms after the addition of 26 g carbon, and at about 80 g addition, carbon is even dissolved in the metal phase. At about 90 g carbon addition, the silica reduction to metallic silicon which is collected in the metal phase starts, and at about

96 g carbon addition, the reduction to titanium slightly begins (threshold 0.1 wt%).

The slag must not be contaminated by the used refractory, and the aim of all the experiments was a complete reduction of iron oxide. Therefore, the raw material was smelted in a graphite crucible with the dimensions of 150/120 mm outer/inner diameters and 200 mm depth. To minimize the graphite consumption of the crucible due to the carbon absorption by the slag and to cover the melt from reoxidizing at the surface, approximately 200 g (depending on the hematite content of the raw material) of lignite coke with a grain size less than 1 mm has been fed together with 3200 g of predried and lumpy raw material of a particle size 10–30 mm. All experiments were conducted

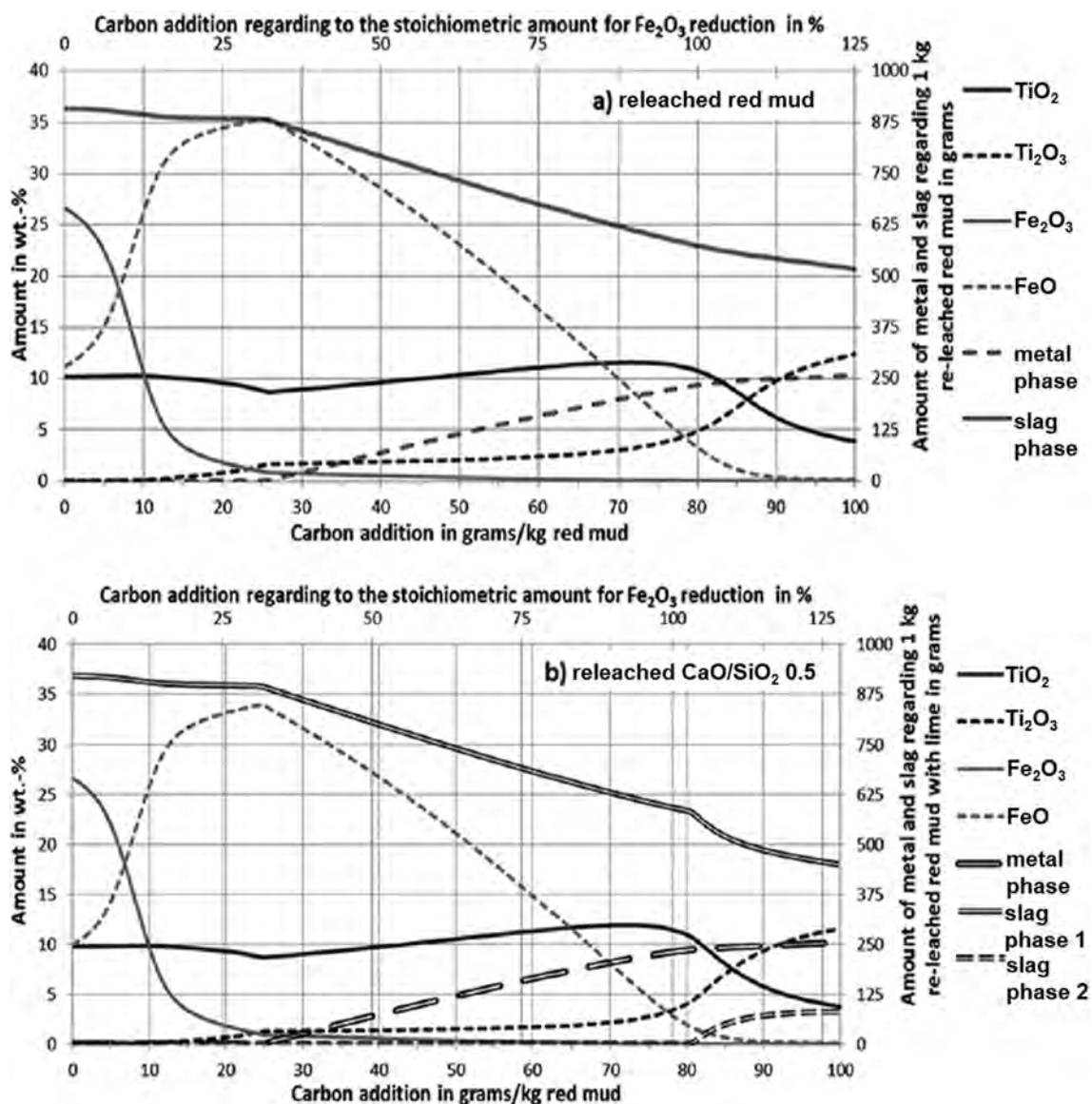


Fig. 16 Component distribution of oxides and sub-oxides during the reduction of **a** re-leached red mud, and **b** re-leached red mud with lime addition calculated at 1650 °C

in a tiltable AC electric arc furnace, which is presented in Fig. 17. Although the setup with one top electrode made of graphite in combination with a water-sprayed copper bottom electrode is typical for DC mode, the furnace was driven without a rectifier. In order to establish a good electric contact, a thin layer of graphite powder was put between the bottom electrode and the graphite crucible. The electric power applied during the smelting process was 12–15 kW. A process temperature of 1600 °C was employed and controlled discontinuously by a pyrometer. Actually, the temperatures varied from 1600 to 1700 °C. The feed rate of the input material was maintained constant at 2500 g/h. After 90 min, the whole material has been fed, and the melt was kept on hold for additional 10 min to complete the hematite reduction. Afterward, the entire melt was tapped into a steel mold, in which metal and slag phase were separated due to the settling behavior of the metal droplets of higher density.

After the carbothermic reduction of red mud, the hazardous residue from the Bayer process, a salable pig iron with about 4 wt% carbon and less than 0.5 wt% silicon and 0.2 wt% titanium can be obtained. The slag is by the addition of lime adjustable in its viscosity, and the sodium content can be varied by adjusting the length of the reduction time. An important role during the reduction process is played by the slag viscosity, since many reduction products like CO, Na, and SiO are in the form of gaseous species and have to pass through the melt. At high viscosities, the ascent of gas bubbles is hindered and forms a foaming slag. The addition of lime during the prior leaching step influences the process handling in the smelting step positively by decreasing the slag viscosity, which was obvious during the experiments. Unfortunately,

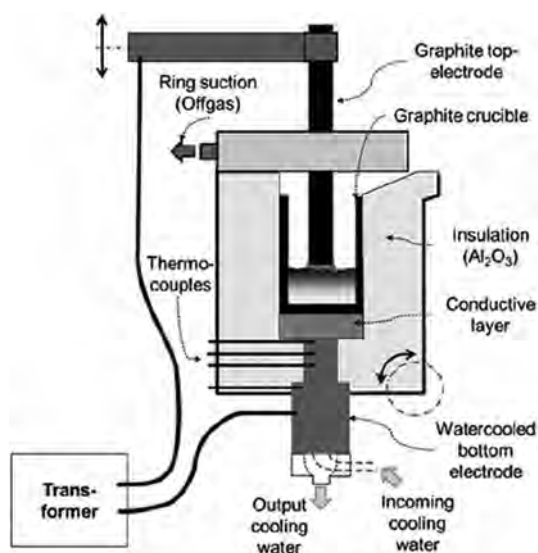


Fig. 17 Sketch of the laboratory electric arc furnace

the calculation of the viscosity is not that easy because the high content of titania in trivalent and tetravalent states is not exactly defined in any known model for slag viscosities. However, FactSage[®] states the viscosities of all slags in the range of 0.27–0.36 Pa × s have positive effect on lowering the viscosity by the addition of lime even though lime increases the liquidus temperature in the range of 100–1500 °C.

Cobalt Recovery from Copper-Smelter Slags [15]

In January 2001, Chambishi Metals commissioned a 40 MW DC arc furnace using selective carbothermic reduction for processing reverberatory furnace slag stockpile of 20 million tons containing 0.34–4.5% cobalt and an average of 1.1% copper. Cobalt occurs as fayalite, whereas copper occurs as oxide and sulfide. An atomizer unit to atomize furnace product—molten Co/Cu/Fe alloy—and a pressure oxidation leach process to leach cobalt and copper and separate iron as goethite was also commissioned. Cobalt- and copper-containing solution is processed in the refinery for production of metals. Commercial application of the DC arc furnace on smelting of copper smelter slag was unique and therefore required an extensive literature search to broaden the knowledge of the theory and the practice.

Mineralogical analysis of the slag carried out by MINTEK, RSA, shown in the Table 2, indicates that the cobalt is present as fayalite (Iron Silicate Matrix), whereas copper is present as oxide, sulfide, and metal. The presence of significant levels of sulfide and metallic copper is due to entrained losses.

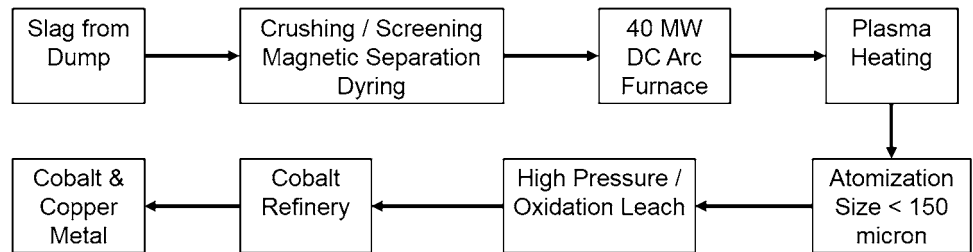
According to the 40 MW DC Arc furnace commissioned in the year 2001, the Chambishi operation's flow sheet is shown in Fig. 18. The slag is excavated from the dump, crushed, and screened to +6, –16 mm particle size; beneficiated to high grade the furnace feed by 15–20%; and dried to reduce moisture to <1%, which is finally fed to the furnace. Furnace product is an alloy of cobalt, copper, and iron. Molten alloy is tapped and atomized to <150 micron particle size which is pumped into the pressure/oxidation leach plant for leaching cobalt and separating iron as goethite. The leaching solution containing cobalt, copper, and other trace impurity elements is processed in cobalt refinery for cobalt and copper metal production.

The furnace was experiencing severe power fluctuations which caused erratic feed rates. This resulted in difficulties in controlling slag bath temperature in the range of 1500–1550 °C. Overfeeding was causing cooling of the bath, whereas underfeeding was causing high temperature, both changing the resistance. This frequent swing in the bath resistance triggered the electrode movement to

Table 2 Mineralogical composition of the Rokana reverberatory slag

Group total Co	Mineral phases	% of total Cu	% of total Co
Slag	Fe, Ca, Al (Mg, K, Co, Cu)—silicates	46.6	94.6
Spinel	Fe(Al, Cr, Ti, Ca, Co, Cu)—oxides	1.1	5.2
Sulfide	Cu(Co, Fe)—sulfide	39.3	0.2
Metal	Cu(Co, Fe)—metal	13.0	< 0.1
	Total	100.0	100.0

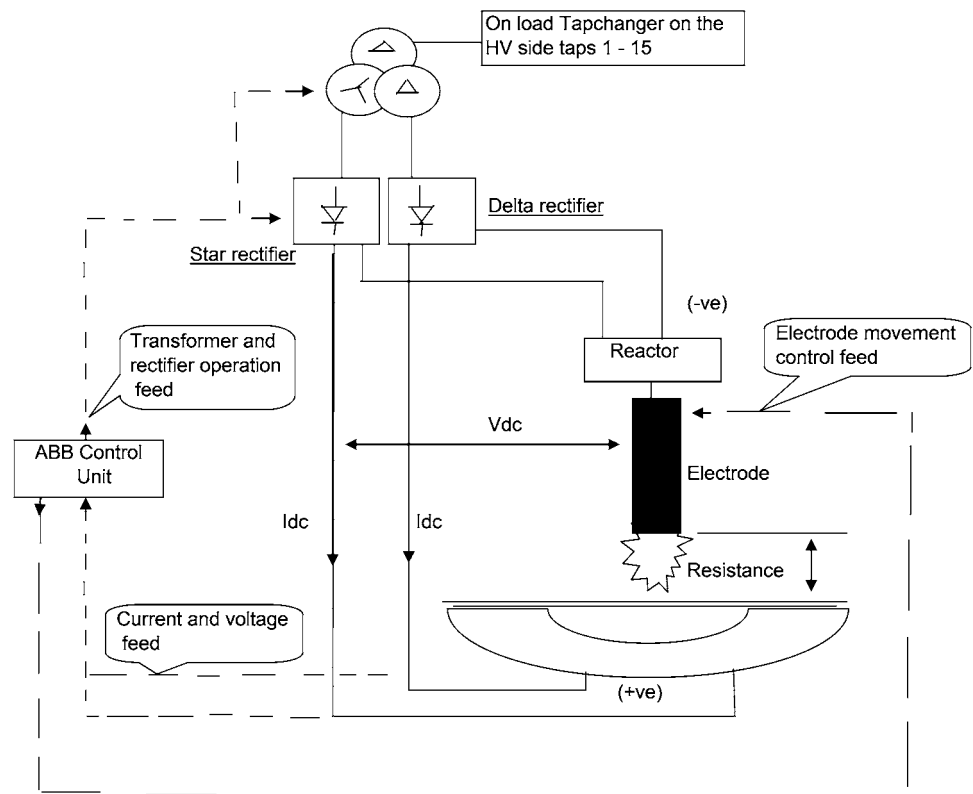
Fig. 18 Simplified flow chart of Chambishi operation after 2001



maintain power set point, causing power fluctuations. Figure 19 shows the circuit control diagram originally built in PLC. The power fluctuations were experienced due to a sudden drop in resistance causing the power to begin to drop. The controller would try to compensate by increasing the current, thus maintaining the power at the set point, until it eventually reached a maximum limit for the tap position. Once the current reached the maximum limit, then the power would fall in line with the resistance. Under

these circumstances, the tap changer should tap down, thus increasing the allowable current. The ABB Group (well known industrial supplier of electronic controls and regulators) controller prevented the transformer from tapping down below tap 10. This was designed to limit the maximum current such that the current density remained under 300 A/m², as specified by the supplier. The ABB was convinced to remove the tap changer control from their

Fig. 19 Schematic electric/control diagram for electrode movement for power control



custom PLC. Chambishi then engineered this functionality into the Plant Scape control system.

The advantage of this change was that Chambishi had the flexibility to alter the philosophy while retaining the integrity of the safety features built into the ABB control system. The Plant Scape system requests a tap changer from the ABB system, which executes it if it is safe to do so. The maximum limit for current was set at 70 kA (250 A/m^2). This meant that the tap setting could safely go down to position 3 (Fig. 20) with no safety risks to electric equipment.

After this change was effected to stabilize the power, the standard deviation improved to 0.84 from 1.6 in the year 2005, indicating a significant improvement as shown in Fig. 16. The standard deviation improved from 1.6 to 0.847 by the end of the year 2006. The standard deviations are calculated for 6 monthly averages at 40 MW power only. The relevant data are graphically shown in Fig. 21.

Valorization of Pb-Containing Slags [16]

The lead and zinc contents of slags from lead production vary depending on the type of the production process and the process parameters. A slag from an oxidation step of crude lead production has a lead content of 50% or more, whereas a slag from a reduction step usually lies below 6% lead and 18% zinc. Therefore, one motivation for a subsequent treatment of the slag is to increase the metal yield of the production line, and by doing so, to increase the profitability of the process. If the metals contained in the otherwise discarded slag are regained and transferred into a product this can decrease the use of primary resources and thus increase the sustainability of lead production. This in turn can achieve or add to a positive company's perception of the public. Figure 22 shows industrial Pb and Zn winning processes in comparison along with the resulting typical Pb/Zn contents in the process slags.

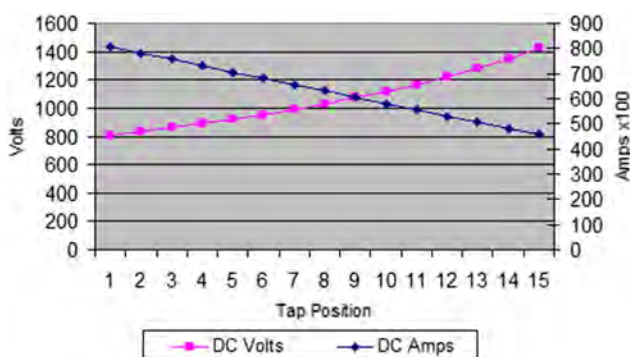


Fig. 20 Voltage and current limits for tap positions, 1–15 (Color figure online)

Facts about lead winning processes are published only fragmentary and intermittent. On the basis of the 2012 minerals yearbook for lead by the USGS [17] and the 2010 lead smelter survey [18], it is possible to estimate the amount of slags that have been produced in 2008 after the reduction step of crude lead winning by smelters that treat only primary feed material or a mixture of primary and secondary feed materials. On the basis that in 2008 the world lead production from primary sources is 3.9 million tons which represents a share of 75% in the primary and primary/secondary smelter's lead production, and that 3% of the lead input of these smelters is lost in the slag, it can be calculated that the amount of slag is 5.3 million tons for 2008. If it is assumed that these slags contain in average 3% lead and 10% zinc, the lead amount in the slag is 160,000 tons, and zinc amounts to 530,000 tons. Together, the metal value equals 982 million Euros. If all of these slags would have been treated toward a final slag with 0.1% lead and 1% zinc, more than 150,000 tons of lead and 370,000 tons of zinc could have been recovered, which represents a metal value of 751 million tons. In 2013, the lead production was 20% higher than in 2008, and therefore, lead and zinc contents entrained in the slags will be considerably higher as well.

The slag fuming process and, to a minor extent, the ISA/Ausmelt process are the standard processes for the treatment of lead slags from crude lead production. Slag fuming takes place in a rectangular water-cooled furnace and is usually carried out batchwise with durations from 30 min up to 3 h per batch. By injection of pulverized carbon and air, an active gas–slag interface is established that can be twenty times the size of the furnace surface. At temperatures between 1150 and 1300 °C, lead and zinc contents are reduced and volatilized from the slag and subsequently oxidized with additional air over the melt, so that they can be recovered in the flue dust as oxides. The slag produced by fuming typically contains 0.5–1.5% lead and 2–4% zinc. The main disadvantages of the process are that lower zinc contents are not possible due to the risk of iron reduction and that it produces large amounts of off-gas and waste heat that have to be treated.

There are some publications about the possibility of using an electric arc furnace or plasma furnace for the treatment of slags, but its main use still is as holding or settling furnace. Nevertheless, electric arc furnaces offer multiple advantages for a slag treatment:

- High versatility in terms of feed material (e.g., solid/liquid), processing mode (e.g., EAF/SAF/SRF, etc.), and parameters (e.g., temperature; continuous/batchwise)
- Small off-gas volume
- Little space required

Fig. 21 Furnace power set point versus actual power (Jan 04–Jan 07) (Color figure online)

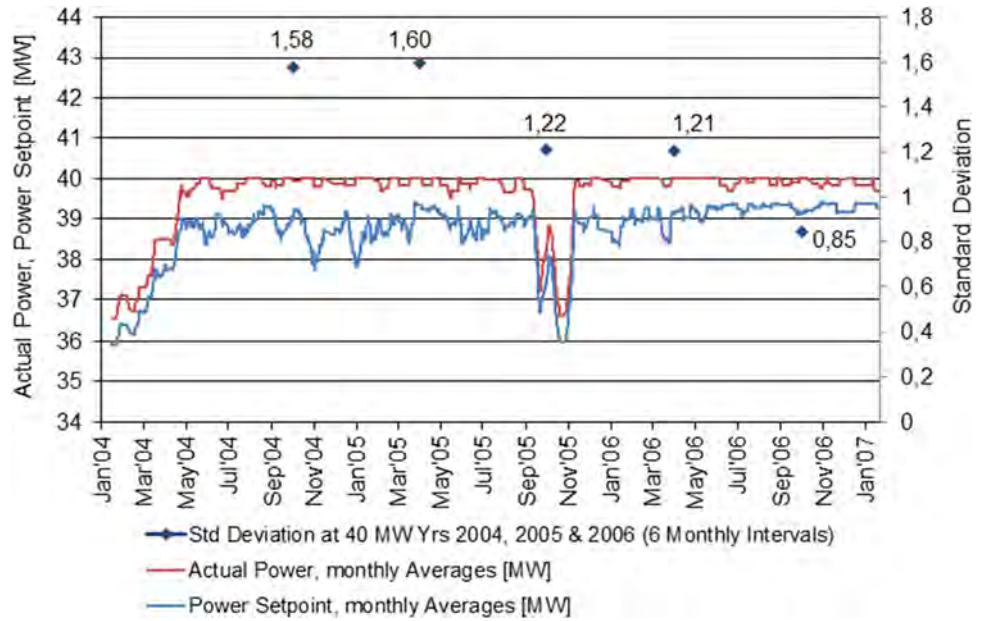


Fig. 22 Comparison of relevant lead winning processes with lead and zinc contents of the produced slags (Color figure online)

	conventional	direct wining			
crude lead winning	SM		ISA / Ausmelt	SKS OBBF	Kivcet
oxidation		QSL	50 % 6 - 10 %	46 % 10 %	(FS + EF)
reduction	BF 1.5 % 11 %	ISF 2.5 % 16 %	3 - 6 % 8 - 16 %	SKS OSBF 2 % 16 %	6 % 18 %
slag cleaning	FF	ISA / Ausmelt		FF	FF
reduction	0.1 % 3 %	1 % 6 - 8 %		0.5 - 1.5 % 2.5 - 4 %	0.1 % 2 %

X process / furnace
X not employed in all installations
y % Pb-content of slag
z % Zn-content of slag

SM: sinter machine
 BF: blast furnace
 ISF: Imperial smelting furnace
 OBBF: Oxygen-Rich Bottom-Blowing Furnace
 OSBF: Oxygen-Rich Side-Blowing Furnace
 EF: electric furnace
 FS: flash smelter
 FF: fuming furnace

- High energy density and high space–time efficiency

On the contrary, the disadvantages are low turbulences in the bath and a high demand of electric energy which can require an expensive electric infrastructure. In this work, it has been investigated if the electric arc furnace is a viable

alternative for the treatment of lead slags. It can be added into an existing process line with only little demand for space and off-gas treatment. It certainly makes best sense to process the liquid slag inline of the main process, but there still is the option to feed solidified slag and to melt it

before treatment, too. In any case, the electric arc furnace is able to adjust the slag temperature as needed. It is possible to generate stronger reducing conditions than in the slag fuming process, because if iron is reduced to metallic state, it can be molten and consumed as reducing agent. This should enable the electric arc furnace to produce slags which are low both in lead and zinc.

Experimental

On the basis of the results of the preparatory work, a series of test runs in a 500-kW pilot-scale DC electric arc furnace have been conducted. In total, more than six tons of six different industrial lead slags have been treated in 25 tests. The aim was to reduce the lead content to less than 0.1% and the zinc content to less than 1%, and thereby to confirm and if possible extend the findings of the previous work, so that a scale up into commercial scale is possible. A schematic of the furnace is depicted in Fig. 23.

Table 3 presents the initial chemical compositions of the slags treated at pilot scale at IME. In addition, the average trial results are given in terms of final Pb and Zn concentrations in the slags. The methods of coke additions to the melt are furthermore mentioned.

Despite the partly insufficient results (in terms of the final lead and zinc contents), important correlations can be derived from the test runs. At first, all test runs show a comparable interdependence of the zinc content upon the lead content throughout the duration of the test runs. Figure 24 shows an exemplary test run with slag type I. The lead content in the slag decreases faster than the zinc content (left). This could be expected, but more interesting is that the decline of the zinc content shows a logarithmic dependency on the lead content of the slag (right).

In consideration of the empirical variation in the samples, this dependency can be found in all the test runs. For each slag type, the logarithmic correlation between lead and zinc is unique, so that by averaging the logarithmic functions of the slag types, one mean function for each slag type can be obtained. Generally speaking, all of these trends can be expressed by an equation of the form:

$$Zn_t = f(Pb_t) = A \cdot \ln(Pb_t) + B \quad (19)$$

where Zn_t is the Zn content in % at time t , Pb_t is the Pb content in % at time t , A is the factor, and B is the constant.

Altogether by calculating the factors A and B , the time-dependent Zn concentration in relation to the Pb content may be expressed as

$$Zn_t = Zn_0 - (-0.01953 \cdot Pb_0 + 4.455 - 0.0063 \cdot Pb_0^2 + 0.5552 \cdot Pb_0 - 3.436) \cdot \ln(Pb_t/Pb_0)$$

Summarizing Remarks

The first SAF was commissioned 100 years ago in Germany. Since then a tremendous development of this smelting tool was recognized all over the world, and submerged arc furnaces (SAF) are now operating in at least 20 different main industrial fields. In metallurgical production, the traditional aim of the SAF is to optimize recovery of metals from slags to the maximum. SMS group has supplied numerous furnaces for this application. Especially in the field of rectangular furnace technology, the SAF could enhance its market position for slag cleaning.

The last order in rectangular furnace for the First quantum project at Kansanshi, Zambia demonstrates convincing results and confirms the intelligent solution (such

Fig. 23 Schematic of the “old” pilot-scale EAF at IME

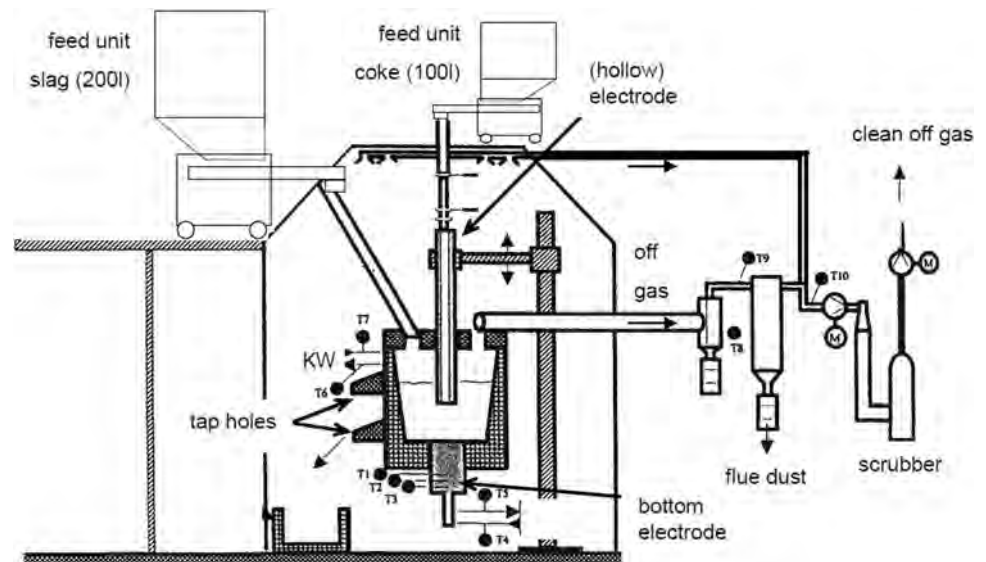


Table 3 Compositions of treated slags and average final experimental results from 25 trials

Slag type	Pb [%]	Zn [%]	Fe [%]	S [%]	SiO ₂ [%]	CaO [%]	MgO [%]	Al ₂ O ₃ [%]
I	8.9	11.7	28.2	0.1	25.1	9.8	1.3	2.3
II	1.1	5.1	25.5	2.6	24.6	16.4	4.4	7.9
III	55.3	5.9	10.3	0.1	7.1	3.4	0.4	0.7
IV	54.4	7.7	9.5	0.4	7.4	3.1	–	–
V	6.8	12.4	23.4	0.3	23.5	9.9	2.2	2.4
VI	5.8	11.4	24.5	0.4	23	10.8	1.5	2.8

Slag type	Method of coke feeding	Number of test runs	Final slag			
			Pb [%]		Zn [%]	
			Average	Best	Average	Best
I	h. el.	6	0.80	0.08	3.50	0.10
II	h. el.	7	0.12	0.02	0.24	0.10
III	h. el.	3	16.6	0.29	0.09	0.05
IV	pre.	2	5.85	3.30	1.44	1.36
V	h. el.	1	0.39	0.39	2.98	2.98
VI	p. i.	4	0.78	0.38	6.09	3.89
	p. i.	2	0.49	0.32	2.94	2.49

h. el. hollow electrode, *pre* premixed (slag & coke), *p. i.* pneumatic coke injection

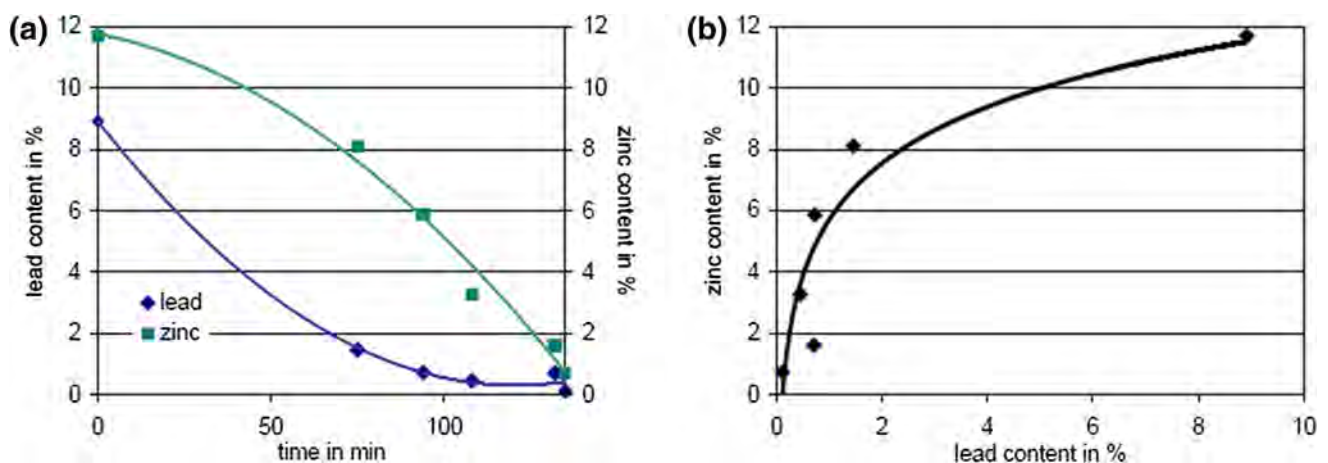


Fig. 24 Slag type I: lead and zinc contents versus duration of a test run (left), and zinc content versus lead content (right) (Color figure online)

as sidewall cooling system, furnace integrity). The incorporation of stirring reactor as a new unit in the copper production line provides new dimensions in the industrial improvement of the iron silicate product, commonly only named slag. With the copper content in the byproduct slag being able to be reduced by 30–50%, depending on the starting raw materials, the raw material copper is better exploited. Furthermore, additional byproducts, which are unwanted for reuse of the iron silicate product, are to some extent even more significantly reduced than copper.

Furthermore, over the recent decades, the SAF has taken a predominant position in nonferrous metallurgy research. Numerous dissertations have been published, which

underline the versatility of this type of furnaces in a variety of industrial and scientific applications. Some examples of recent scientific results have been demonstrated. The applications for SAFs range from the reuse of previously landfilled red mud, cobalt-recovery operations, and the reduction and removal of Pb and Zn from slags, to future potential applications, for example, in the pyrometallurgical treatment of deep-sea minerals such as polymetallic Mn-nodules.

Two process routes are generally applied for slag cleaning. The first is the grinding followed by flotation, and the second is the slag cleaning in an (electric) furnace. Popularity of either option has fluctuated over the years,

and currently the milling–flotation route seems to be the more popular option.

Electric slag-cleaning furnaces have been chosen not only based on economic aspects but also based on the reason that, at almost all locations in the world, the environmental sensibility is gaining more importance. This pertains to the air pollution as well as to applications where slag is used as a landfill material.

Therefore, in some cases, the electric furnace is a substitute for the existing slag-cleaning processes being energized by fuel causing high emissions of gas and which are less efficient regarding the metal recovery.

The majority of ferroalloys are produced by pyrometallurgical smelting in submerged arc furnaces. The hydrometallurgical production of ferroalloys such as high-pressure acid-leaching processes for nickel production have so far not shown the predicted economic and technical benefits.

The SAF-based solutions are not only environmentally balanced, but also economically feasible. The economics of this unit are for some applications outstanding. Taking the example of conventional plant utilizing submerged arc furnace for copper slag cleaning and taking the current copper price of approximately 5000 USD per ton of copper and a copper production of approximately 200,000 tpy, such a unit will have an amortization period of less than 1 year. From a technological point of view, even bigger units are possible but their economic feasibility has to be carefully ascertained.

The close cooperation between University researchers and experienced industry engineers is fundamental to the advancement and optimization of industrial processes. The cooperation between SMS and IME shows that the entire size spectrum from lab-scale and technical scale up to pilot- and industry-size research may be realized and leads to important process improvements. In general, it was shown that the application of the submerged arc furnace technology to the valorization of slags enables the production of low-level heavy metal contamination of the slags while simultaneously allowing the recovery of valuable metals from the slags.

Compliance with Ethical Standards

Conflict of interest The authors declare that they have no conflict of interest.

References

- Kempken J, Degel R (2005) A hot technology. *Met Bull Mon*, pp 23–26
- Degel R, Kunze J, Oterdoom H, Wübbels T, Kempken J (2007) Rectangular furnace design, furnace modelling and slag washing machine for the non-ferrous industry. In: *European Metallurgical Conference (EMC) Proceedings 2007*, GDMB, Düsseldorf, Germany. ISBN 978-3-940276-08-7
- Degel R, Kunze J (2003) History, current status of submerged arc furnace technology for ferro alloy metals. *Steel Grips* 1(3). <https://www.steel-grips.com/>
- Kempken J, Degel R (2006) 100 years of SMS demag submerged arc furnace technology. In: *World of metallurgy—ERZMETALL*, vol 59, no 3, pp 143–151. ISSN 1613-2394
- Warczok A (2003) SAF fundamentals, stage I. Universidad de Chile, Santiago
- Oeters F (1989) *Metallurgie der Stahlherstellung [Metallurgy of steel making]*. Springer, Berlin, p 880. ISBN 3-540-51040-0
- Volkert G, Frank KD (1972) *Metallurgie der Ferrolegierungen [Metallurgy of ferro alloys]*. Springer, Berlin. ISBN 978-3540052029
- Degel R, Kunze J, Oterdoom H, Warczok A, Riveros G (2009) Computer simulator of slag cleaning in an electric furnace. In: *Proceedings of Copper 2007. The Carlos Diaz Symposium on Pyrometallurgy*, Toronto, Canada, pp 367–378. ISBN 978-1-894475-73-0
- Grigoryan V, Belyanchikov L, Stomakhin A (1989) *Theoretical principles of electric steelmaking*. Mir Publishers, Moscow
- Degel R, Kunze J, Kalisch M, Oterdoom H, Warczok A, Riveros G (2009) Latest results of the intensive slag cleaning reactor for metal recovery on the basis of copper. In: *Proceedings of Copper 2010*, GDMB, Hamburg, Germany, pp 1213–1232. ISBN 978-3-940276-32-2
- Kunze J, Degel R, Borgwardt D, Warczok A, Riveros G. Method and device for extracting a metal from slag containing the metal. Patent: WO/2006/131372
- Zander M, Friedrich B, Schmid J, Hoppe M, Degel R, König R (2013) Efficiency of slag cleaning in a magnetically induced stirring reactor. In: *European Metallurgical Conference (EMC) Proceedings 2013*, GDMB, Weimar, Germany. ISBN 978-3-940276-52-0
- König R, Weyer A, Degel R, Schmid J, Kadereit H, Specht A (2013) Highly efficient slag cleaning—latest results from pilot-scale tests. In: Kvithyld A et al (eds) *REWAS 2013*. Springer, Cham. https://doi.org/10.1007/978-3-319-48763-2_1
- Kaußen F, Friedrich B (2015) Reductive smelting of red mud for iron recovery, *Chemie Ingenieur Technik (CIT)*, ISSN: 1522-2640, vol 87, no 11. Wiley, New York. <https://doi.org/10.1002/cite.201500067>
- Singh HP. Implementation of a novel technology for the recovery of cobalt from copper smelter slags (at Chambishi Metals Plc, Zambia). Dissertation 2012, RWTH Aachen University, p 909. ISBN: 978-3-8440-0960-6
- Böhlke J. Behandlung von Schlacken der Bleigewinnung im Elektrolichtbogenofen [Treatment of slags from Pb production in an electric arc furnace]. Dissertation 2016, RWTH Aachen University, p 913. ISBN: 978-3-8440-4763-9
- Gubernan DE (2012) *Minerals yearbook: lead* (advance release). U.S. Department of the Interior, U.S. Geological Survey. ISBN 978-1-4113-3349-9
- Hayes PC, Schlesinger ME, Steil H-U, Siegmund A (2010) Lead smelter survey. In: *PbZn 2010: Proceedings of Lead-Zinc 2010*, Vancouver, Canada. Wiley, New York. ISBN 978-0-470-94315-1
- Kempken J, Degel R, Schreiter T, Schmieden H (2006) History and innovation of SMS Demag smelting technologies. In: *Proceedings of the 2nd International Platinum Conference “Platinum Surges Ahead”*, SAIMM, Sun City, South Africa
- Warczok A (2003) SAF fundamentals, mathematical model of copper slag cleaning. Universidad de Chile, Santiago